Applied Physics Letters ARTICLE scitation.org/journal/apl

Experimental evidence of the Poisson-like effect for flexural waves in thin metallic plates

Cite as: Appl. Phys. Lett. **120**, 094102 (2022); doi: 10.1063/5.0080450
Submitted: 1 December 2021 · Accepted: 14 February 2022 ·
Published Online: 28 February 2022

View Online Export Citation CrossMark

José Sánchez-Dehesa,[1,a)] Penglin Gao,[1,b)] Francisco Cervera,[1] Alberto Broatch,[2] Jorge García-Tíscar,[2] and Andrés Felgueroso[2]

AFFILIATIONS

[1]Wave Phenomena Group, Department of Electronic Engineering, Universitat Politècnica de València, Camino de vera s.n. (Building 7F), ES-46022 Valencia, Spain
[2]CMT-Motores Térmicos, Universitat Politècnica de València, Camino de vera s.n. (Building 6D), ES-46022 Valencia, Spain

Note: This paper is part of the APL Special Collection on Acoustic and Elastic Metamaterials and Metasurfaces.
[a)]**Author to whom correspondence should be addressed:** jsdehesa@upv.es
[b)]**Present address:** State Key Laboratory of Mechanical System and Vibration, Shanghai Jiao Tong University, 200240 Shanghai, China.

ABSTRACT

This Letter reports the feasibility of a structure specifically designed for the control of flexural waves propagating in thin perforated plates. The structure, here denominated as a redirector device, consists of a square array of free holes that splits the impinging beam and transmits sideways their vibrational energy. This behavior is known as a Poisson-like effect, and it was theoretically described in different acoustic structures. This effect is experimentally demonstrated for flexural waves excited in an aluminum perforated plate, and it is explained in terms of a physical mechanism different to that reported for acoustic waves interacting with thin hollow cylinders embedded in water. In addition, a collimator device based also in free holes is designed and validated with the purpose of providing the beam impinging the redirector device. The measurements indicate that the amount of redirected energy is strongly enhanced when a barrier of two-beam resonators is added at the rear side of the redirector. All the designs are validated by an experimental setup employing 1 mm thick aluminum plates.

The redirection of classical waves appears in different physical phenomena in nature. In electromagnetism, a canonical example is provided by the Snell's law, which describes the redirection appearing when electromagnetic waves cross an interface separating two different dielectric media. In acoustics, a similar phenomenon is represented by the deflection of sound propagating through an acoustic medium, such as the atmosphere, with a gradient of temperature. At normal incidence, however, the impinging waves will pass through a flat interface directly without any deflection. Recently, the control of wave propagation has become a hot topic due to the development of the metasurfaces,[1] artificial structures providing novel degrees of freedom facilitating the manipulation of classical waves.

The redirection of normal incident waves to the perpendicular sides is interesting not only from a fundamental point of view but also for its practical applications in the control of vibrations. For example, in a lattice of perforated cylindrical shells, one can employ the wave redirection to increase the propagation path of sound inside the lattice and, therefore, enhance the dissipation loss produced by the absorbing units in the lattice. The redirection in these structures was explained by Garcia-Chocano and Sánchez-Dehesa[2] in terms of the excitation of a leaky guided mode propagating normally to the incident direction. Two years later, Bozhko *et al.*[3] developed a model explaining the redirection of acoustic waves impinging a linear chain of perforated shells in air. They validated that the redirection of waves to $\pm 90^\circ$ with respect to the incident direction is due to the excitation of a guided eigenmode along the linear chain. They also demonstrated that, at oblique incidence, the sound waves are redirected to only one side along the periodic chain depending on the symmetric or antisymmetric character of the eigenmode resonantly excited. Almost simultaneously, Titovich and Norris[4] described a redirection of acoustic energy to $\pm 90^\circ$ studying arrays of thin elastic shells in water. This result was denominated as a Poisson-like effect and was explained in terms of a different physical mechanism involving the excitation of a quadrupole resonance of the cylindrical shells. This effect, which has not been experimentally supported to date, can be also expected for cylindrical shells embedded in air since Kosevich *et al.*[5] predicted that

the excitation of quadruple resonances is also possible in air when the thickness of the thin-walled hollow cylinders accomplishes a given relationship with the material parameters of the cylinders. In 2017, Bai *et al.*[6] demonstrated an extraordinary lateral beaming of sound using a finite square-lattice phononic crystal and they explained the observed behavior in term of the equivalence of the states located around the first Brillouin zone. More recently, Su and Banerjee[7] reported an extraordinary lateral sound beaming effect in a phononic crystal composed of Willis scatterers arranged in a square lattice pattern. The asymmetric lateral beaming effect was possible thanks to the matching of the antisymmetric and symmetric modes to the second-order Bragg scattering in the Willis medium.

For the case of flexural waves, Gao *et al.*[8] predicted that the redirection of flexural waves is possible by using a cluster of free holes distributed in a square lattice and perforated in a thin metallic plate. The spectral problem for flexural vibrations of a thin elastic plate containing a square lattice of free holes was first addressed by Movchan *et al.*[9] This type of periodically perforated structures was denominated as platonic crystals by McPhedran *et al.*,[10] a name that it is employed along this work.

By carefully studying the guide modes of selected finite platonic crystal consisting of circular free holes, Gao *et al.*[8] show that, at normal incidence, the lowest order symmetric leaky guide mode (S0 mode) can be excited and can produce the splitting of incident wave in two orthogonal directions, i.e., producing the so-called Poisson-like effect.

This Letter presents experimental evidence, showing that the redirection to the lateral sides is feasible by using a structure named as redirector, which consists of twenty-one holes drilled by laser-cutting in an aluminum plate 1 mm thick. For a practical demonstration, we have developed another structure of holes, here denominated as collimator, that transforms a point source of flexural waves into an output collimated beam. This beam is later employed as the source of flexural waves impinging the redirector. In addition, it will be shown that the amount of vibration energy transmitted sideways by the redirector can be enhanced by suppressing the ballistic transmittance through the redirector device. This suppression is obtained by a platonic crystal barrier made of twenty-seven two-beam resonators specifically designed with a bandgap in the working frequency of the device. The measurements here reported validate the feasibility of the proposal in Ref. 8 and open the possibility of designing more complex structures with the goal of controlling the propagation of flexural waves in metallic plates.

The structures presented below have been designed using the biharmonic equation, which is based on the Kirchoff–Love plate theory, and it describes well their interaction with lattices of holes and inclusions.[11] The resulting semi-analytical algorithm was extended to the case of N-beam resonators,[12] and it has been applied here to design the structure of two-beam resonators acting as a barrier to the flexural waves crossing the redirector structure. The scattering properties of the waves interacting with the structures under study have been obtained in the framework of the multiple scattering formalism reported in Refs. 13 and 14. The accuracy of this simplified approach has been validated by its comparison with published results[15] and with complex three-dimensional (3D) numerical simulations based on finite elements using a commercial package (COMSOL multiphysics) where the 3D full elastic equations were taken into account.[13]

The structures are designed following a two-step process. First, the simplified algorithm is employed to obtain the parameters defining the structures with the requested performance. Remember that the algorithm is subjected to the limitations of the Kirchhoff–Love and the Euler–Bernoulli theories and, therefore, only provides out-of-plane vibration features. However, it has large computational advantages, allowing the determination of the optimum parameters of a given structure with minimum time. Once the structure is determined, in the second step, we validate it by using the 3D solid mechanics module of the commercial package COMSOL multiphysics. Perfectly matched layers (PML) are applied in the x- and y-directions in order to avoid undesired reflections at the boundaries of the calculation region. Let us point out that figures reporting the calculated out-of-plane displacements are obtained from the corresponding 3D numerical simulations.

In the calculations, we consider that the arrays of holes and resonators are drilled in homogeneous aluminum (Al-5745) plates with the following parameters (provided by the manufacturer): Young's modulus $E = 70$ GPa, Poisson's ratio $\nu = 0.33$, mass density $\rho = 2.7 \times 10^3$ kg/m^3, and plate thickness $h = 1$ mm.

First, we described in brief the design and expected the performance of the collimator device, which is the structure in charge of transforming a point source of flexural waves into a collimated beam. To design the collimator, we have exploited the band structure properties of a platonic crystal consisting of a square distribution of free holes drilled in the thin aluminum plate. A similar procedure was previously employed to demonstrate acoustic collimation by phononic crystals slabs[16,17] and by a stacking holey Plexiglas plates,[18] respectively. An alternative approach essayed in acoustics was applying genetic algorithms to determine the non-periodic distribution of cylindrical rods surrounding the punctual source capable of transforming the omnidirectional source of waves into a highly collimated beam.[19]

We have fixed in 15 kHz the working frequency of the collimator. With this frequency taken as the target, the design process involves the calculation of the flexural bands of platonic structures with different dimensions (i.e., with different lattice parameter, a_c, and hole radius, r_c) until the equifrequency surface predicts a beam guided along the direction of interest. The optimization process is relatively fast thanks to the computational efficiency of the semi-analytical approach described in Ref. 13.

The simulations indicate that the collimator has the desired performance for a lattice of 20×30 free holes with radius $r_c = 5$ mm distributed in a square lattice with period $a_c = 12$ mm. Figure 1(a) shows a snapshot of the out-of-plane displacement field produced by the interaction of the waves excited by the omnidirectional punctual source located at the middle ($y = 0$) of the first column of holes. Together with the beam guided along the line $y = 0$, the two-dimensional (2D) map predicts that two additional beams (blue arrows) arise from the left-hand-side corners of the clusters. These sidelobes, which are also observed inside the collimator, are due to the properties of the underlying band structure associated with the platonic crystal employed as a collimator. They are tilted at about $\pm 45°$ with respect to the horizontal direction and produce undesirable effects on the profile of the central beam when it propagates in the homogeneous region of the plate. Thus, it is shown in Fig. 1(b), where the profile of the beam is depicted at two distances from the collimator surface that for the shorter distance (L_1), the output beam (blue dashed

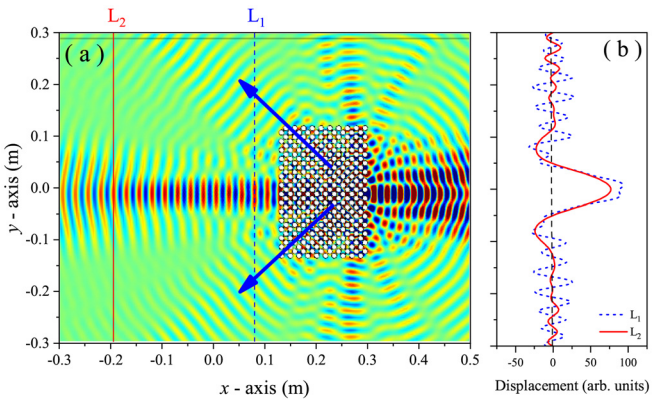

FIG. 1. (a) Snapshot of the out-of-plane displacement field showing the performance (at 15 kHz) of a collimator device consisting of a cluster of free holes (white circles) distributed in a square array. The blue arrows indicate the two sidelobes accompanying the central collimated beam created by the holey array. (b) The profiles of the output beam obtained at 5 cm (L_1) and 35 cm (L_2) from the collimator surface.

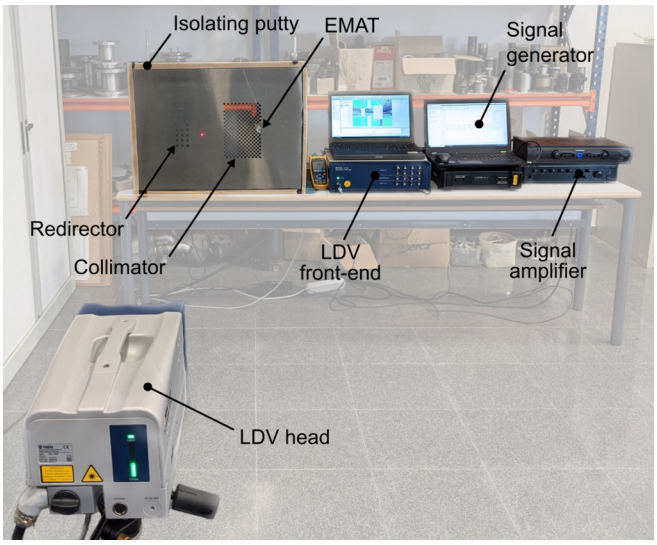

FIG. 2. Experimental setup employed in the measurements of the out-of-plane displacements produced by the flexural waves propagating in the aluminum plate containing the structures of holes resulting from the design procedure.

line) exhibits lateral oscillations that spoils its desired Gaussian-like profile. For the larger distance (L_2), the beam profile shows almost negligible side oscillation and it determines the adequate distance to locate the redirector device. However, in order to have the freedom of placing the redirector closer to the collimator surface, we add two absorbing strips to suppress the unavoidable sidelobes. The strips are located in the region where the main central beam propagates and close to the left-hand-side surface of the collimator. Therefore, in what follows, all the results both numerical and experimental are performed with the absorbing strips providing the suppression of the sidelobes accompanying the central collimated beam.

The array of holes defining the redirector device, responsible of the Poisson-like effect, has been redesigned to fit into the features of the impinging beam provided by the collimator. In the same manner, the enhancement of the Poisson-like effect is achieved by adding a barrier consisting on an array of two-bean resonators, with parameters and dimension slightly different to that described in Ref. 8. See the supplementary material for a detailed account of the design procedure and predicted performance of the structures that are experimentally characterized below.

The performance of the designed structures leading to the Poisson-like effect for flexural waves is validated with the experimental setup described in Fig. 2. The holey structures have been manufactured in aluminum (Al-5745) plates 1 mm thick and with the dimension of about 800 × 600 mm. The holes and the resonators corresponding to the three structures resulting from the designs have been laser-cut in different plates. The laser-cutting technique employed has an accuracy higher than 0.1 mm.

The plate shown in Fig. 2 corresponds to the sample containing the collimator and the redirector. Notice how a mastic tape covers the external edges of the plate in order to avoid wave reflections at the plate borders, thus mimicking the anechoic boundary conditions used in the numerical simulations. Specifically, we have employed a 3M Scotch film Electrical Insulation Putty of 3.175 mm thick and 38.1 mm wide. In brief, the measurements are performed using and audio card of a laptop to synthesize a sinusoidal signal, which is amplified with a 200 W Samson signal amplifier. The amplified electrical signal feeds an electromagnetic transducer (EMAT) made of a coil surrounding a 12 mm diameter cylindrical magnetic core, which is placed close to the plate without touching it. The EMAT excites flexural waves in the plate with the target frequency without any contact between transducer and the plate.

A Polytec PSV-500 scanning laser Doppler vibrometer (LDV) is used to characterize the propagation of the flexural waves excited by the EMAT. Therefore, a complete 2D map of the Z-displacement field in the total area of the plate is obtained without any mass addition, avoiding unintended effects. The interpolation and demodulation techniques incorporated in the LDV reports out-of-plane displacements on the order of picometer (pm). The LDV head is placed at about 2 meters from the surface plate, which is discretized into a scanning grid with the order of 1600 points (avoiding the areas occupied by the drilled structures and the insulating strips). The scan spatial resolution, higher than $3.5 \times 3.5\,\text{mm}^2$, is selected to have at least seven measurements points per target wavelength.

The vibrometer analyzes frequencies from 10 to 20 kHz, with a resolution in the frequency of 3.125 Hz thanks to 3201 FFT lines. In addition, we preserve the phase reference when the laser beam is redirected to the next scanning position. Thus, the LDV records not only the amplitude but also the phase of each measurement point, which are employed later to reconstruct the time evolution of the waves across the whole plate.

In what follows, we show the validation of the structure designed as a collimator, which should be considered a relevant contribution of this work since there is not a similar device for flexural waves reported so far. The measured performance of the collimator has been obtained using the EMAT as an approximate punctual source of omnidirectional flexural waves. Figure 3(a) shows a snapshot of the total Z-displacement field resulting from the interaction of the excited

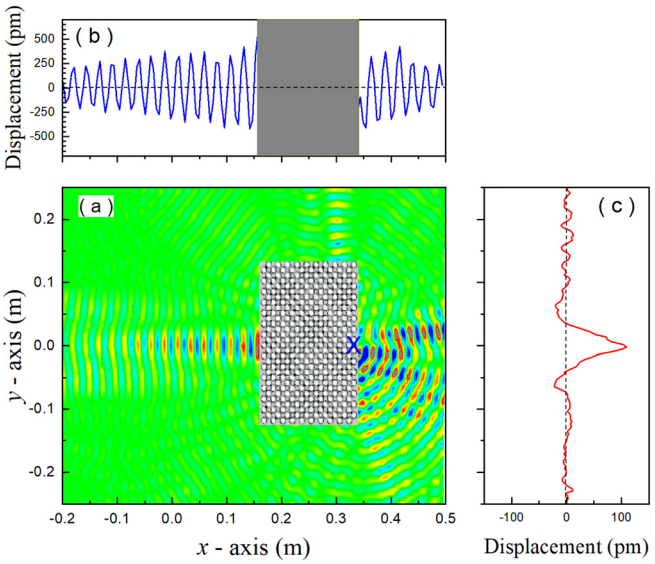

FIG. 3. (a) Snapshot of the measured out-of-plane displacement field demonstrating the performance of the collimator. An image of the holes' structure representing the collimator has been pasted covering the area where no data are acquired. (b) Cut of the displacement 2D map along the horizontal line passing through $y = 0$. (c) The corresponding cut along the vertical line passing through $x = 0.06$ m. The dashed lines in (b) and (c) are guides for the eye, indicating the zero-displacement level.

flexural waves with the collimator. An image illustrating the collimator (white circles) has been pasted in order to cover the area without measurements. The EMAT is located behind the plate, approximately at the middle of right-hand-side column of holes. The output beam arising from the collimator represents the collimated beam resulting from the properties of the flexural band of this platonic structure.

Figures 3(b) and 3(c) represent the profiles of the output beam along the x-axis (with $y = 0$) and along the y-axis (with $x = 0.06$), respectively. It is observed in Fig. 3(b) that the beam has a perfect oscillatory behavior with the decrease in amplitude with the increase in distance from the collimator surface. Moreover, Fig. 3(c) shows that the beam is almost symmetric with respect to the XZ-plane passing through the line $y = 0$. Regarding the waves observed at the right-half-space in Fig. 3(a), they show a clear asymmetric 2D pattern, which is due to the specific features of the excitation source (the EMAT) employed in our setup. Since the EMAT is not punctual, small deviations of its ideal (symmetric) position with respect to the arrays of holes produce the loss of symmetry observed not only in this case but also in the rest of measurements. The supplementary material presents simulations supporting this explanation. The additional beams emerging along the direction $\pm 45°$ are barely seen but do appear in the measurements as it was predicted in the simulations. Motion pictures showing the time evolution of the measured out-of-plane displacement without the absorbing strips and with them are provided in the supplementary material; see SM-video 1 and SM-video 2, respectively. Once we have demonstrated that the collimator can be employed as a device to provide a reasonably collimated beam, the structure of holes defining the redirector device is drilled in another plate together with the collimator.

Figure 4(a) shows a snapshot of the measured out-of-plane total displacement field (real part) where the two sideways-transmitted beams are clearly observed. Two strips of the mastic tape (black areas) are attached to the plate surface to mimic the numerical simulations and, thus, suppress the sidelobes generated by the collimator. Figures 4(b) and 4(c) represent the profiles of the displacement along the horizontal x-axis and along the vertical line defined by the coordinate $x = -0.09$, which crosses the middle column of holes of the redirector. The vertical profile shows that the oscillations of the beams transmitted along the lateral direction are practically the same, demonstrating the Poisson-like effect similar to that predicted for other type of waves.[4] A motion picture showing the time evolution of the measured out-of-plane displacement (real part) at 15 kHz is provided in the supplementary material (see SM-video 3).

Finally, a third plate was manufactured containing the structure of three columns of two-beam resonators acting as a barrier to the horizontal transmitted beam. See the supplementary material for a detailed account of its design. Figure 5(a) shows a snapshot of the measured 2D map (at 15 kHz) of the total out-of-plane displacement field (real part). For visualization purposes, images of the different structures have been pasted to the plot, covering the areas where no measurements were attempted. The two sideway-transmitted beams are now stronger than that observed in Fig. 4(a). The profiles along the horizontal direction defined by the x-axis and the vertical direction defined by the coordinate $x = -0.125$ m are given, respectively, in Figs. 5(b) and 5(c). The experimental data validate the advantage of using a barrier located to the rear side of the redirector to enhance the Poisson-like effect. A motion picture showing the time evolution of

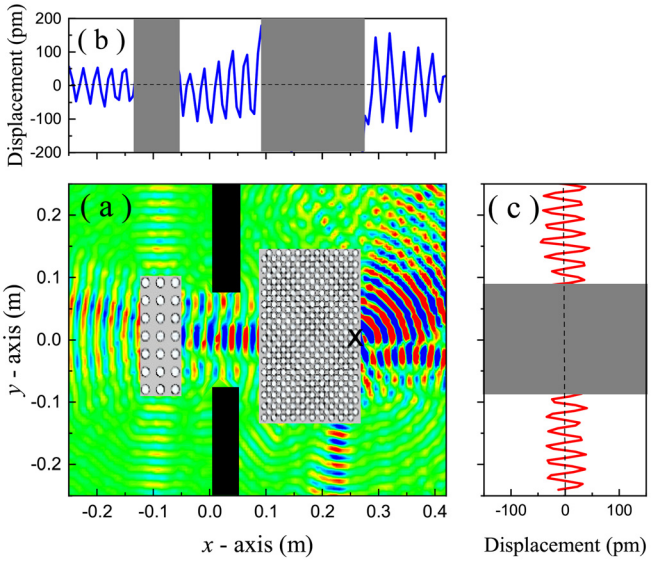

FIG. 4. (a) Snapshot of the measured out-of-plane displacement field demonstrating the performance of the redirector structure. The grayed vertical rectangles represent the mastic tape attached to the surface plate. Images of the collimator and the redirector have been pasted to cover the areas where no data are acquired. (b) Cut in the 2D map showing the profile along the horizontal line passing through $y = 0$. (c) The corresponding profile along the vertical line passing through $x = -0.09$.

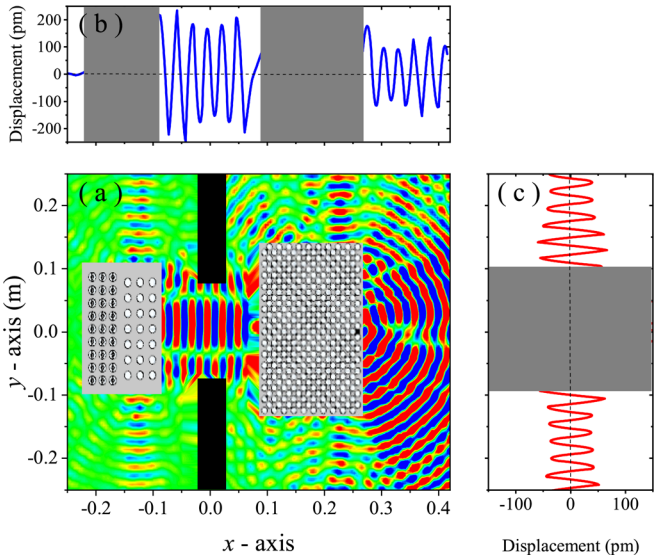

FIG. 5. (a) Snapshot of the measured out-of-plane total displacement field (at 15 kHz) demonstrating the enhancement of the two sideways-transmitted beams when a resonant barrier is added at the rear of the redirector structure. An image of the structures drilled in the plate is pasted to cover the areas where no data were acquired. (b) Profile of the measured Z-displacements along the horizontal line $y = 0$. (c) The corresponding profile measured along the vertical line passing through $x = -0.125$ m. The dashed lines in (b) and (c) are guides for the eye, indicating the zero-displacement level.

the measured out-of-plane displacement (real part) at 15 kHz is provided in the supplementary material (see SM-video 4).

In summary, we have reported measurements demonstrating the feasibility of the Poisson-like effect for flexural waves in thin elastic plates. The interaction of an impinging beam with a specifically designed structure denominated redirector has produced the splitting and the sideways transmission of the vibrational energy in a similar manner than that described in acoustics[4] but caused by a different physical mechanism. The measurements also demonstrate that adding a platonic crystal barrier at the rear side of the redirector allows an enhancement of the amount of energy transmitted sideways. In addition, this work has introduced another interesting device for the control of flexural waves here denominated by a collimator, which has been specifically designed here to generate the beam impinging the redirector device. Let us point out that the experimental data corroborated the predictions obtained by numerical simulations performed with a 2D modeling (thin plate approach) as well as with a full 3D elastic treatment. The structures demonstrated here have many potential applications for the control and guiding of flexural waves propagating in elastic plates. For example, in aeronautic and astronautic industries, these structures can be employed to collimate and redirect waves to specific regions where sensors are located. For the Poisson-like effect, we foresee useful devices for the filtering and splitting of flexural waves at selected frequencies.

See the supplementary material for videos of the out-of-plane displacement measured in the different aluminum plate samples here studied; "SM-video 1" for the collimator, "SM-video 2" for the collimator plus the absorbing stripes, "SM-video 3" for the redirector structure, and "SM-video 4" for the enhanced device containing a barrier at the rear side of the redirector.

This research was partially supported by Grant No. PID2020-112759GB-I00 funded by MCIN/AEI/10.13039/501100011033 and by "ERDF A way of making Europe." J.S.-D. acknowledges the "Proyecto interno" supported by the Universitat Politècnica de València. A.F. is supported through the Programa de Apoyo para la Investigación y Desarrollo of the Universitat Politècnica de València under Grant Nos. PAID-01-20 and 21589. J.S.-D. and P.G. acknowledge useful conversations with Johan Christensen.

AUTHOR DECLARATIONS

Conflict of Interest

The authors have no conflicts of interest to disclose.

DATA AVAILABILITY

The data that support the findings of this study are available from the corresponding author upon reasonable request.

REFERENCES

[1]H. Chen, A. J. Taylor, and N. Yu, Rep. Prog. Phys. **79**, 076401 (2016).
[2]V. M. García-Chocano and J. Sánchez-Dehesa, Appl. Phys. Lett. **106**, 124104 (2015).
[3]A. Bozhko, J. Sánchez-Dehesa, F. Cervera, and A. Krokhin, Phys. Rev. Appl. **7**, 064034 (2017).
[4]A. Titovich and A. N. Norris, J. Acoust. Soc. Am. **139**, 3353 (2016).
[5]Y. A. Kosevich, C. Goffaux, and J. Sánchez-Dehesa, Phys. Rev. B **74**, 012301 (2006).
[6]X. Bai, C. Qiu, H. He, S. Peng, M. Ke, and Z. Liu, Phys. Lett. A **381**, 886 (2017).
[7]X. Su and D. Banerjee, Phys. Rev. Res. **3**, 033080 (2021).
[8]P. Gao, J. Sánchez-Dehesa, and L. Wu, J. Acoust. Soc. Am. **144**, 1053 (2018).
[9]A. Movchan, N. Movchan, and R. McPhedran, Proc. R. Soc. A **463**, 2505 (2007).
[10]R. McPhedran, A. Movchan, and N. Movchan, Mech. Mater. **41**, 356 (2009).
[11]A. Norris and C. Vemula, J. Sound Vib. **181**, 115 (1995).
[12]A. Climente, P. Gao, L. Wu, and J. Sánchez-Dehesa, J. Acoust. Soc. Am. **142**, 3205 (2017).
[13]P. Gao, A. Climente, J. Sánchez-Dehesa, and L. Wu, J. Appl. Phys. **123**, 091707 (2018).
[14]P. Gao, A. Climente, J. Sánchez-Dehesa, and L. Wu, J. Sound Vib. **444**, 108 (2019).
[15]E. Andreassen, K. Manktelow, and M. Ruzzene, J. Sound Vib. **335**, 187 (2015).
[16]L.-S. Chen, C.-H. Kuo, and Z. Ye, Appl. Phys. Lett. **85**, 1072 (2004).
[17]J. Shi, S.-C. S. Lin, and T. J. Huang, Appl. Phys. Lett. **92**, 111901 (2008).
[18]V. M. García-Chocano, J. Christensen, and J. Sánchez-Dehesa, Phys. Rev. Lett. **112**, 144301 (2014).
[19]A. Håkansson, D. Torrent, F. Cervera, and J. Sánchez-Dehesa, Appl. Phys. Lett. **90**, 224107 (2007).